

Density of states in d -wave superconductors of finite size

Ya. V. Fominov^{1,*} and A. A. Golubov^{2,†}

¹*L. D. Landau Institute for Theoretical Physics RAS, 119334 Moscow, Russia*

²*Faculty of Science and Technology, University of Twente, 7500 AE Enschede, The Netherlands*

(Dated: 30 December 2004)

We consider the effect of the finite size in the ab -plane on the surface density of states (DoS) in clean d -wave superconductors. In the bulk, the DoS is gapless along the nodal directions, while the presence of a surface leads to formation of another type of the low-energy states, the midgap states with zero energy. We demonstrate that finiteness of the superconductor in one of dimensions provides the energy gap for all directions of quasiparticle motion except for $\theta = 45^\circ$ (θ is the angle between the trajectory and the surface normal); then the angle-averaged DoS behaves linearly at small energies. This result is valid unless the crystal is 0° - or 45° -oriented ($\alpha \neq 0^\circ$ or 45° , where α is the angle between the a -axis and the surface normal). In the special case of $\alpha = 0^\circ$, the spectrum is gapped for all trajectories θ ; the angle-averaged DoS is also gapped. In the special case of $\alpha = 45^\circ$, the spectrum is gapless for all trajectories θ ; the angle-averaged DoS is then large at low energies. In all the cases, the angle-resolved DoS consists of energy bands that are formed similarly to the Kronig–Penney model. The analytical results are confirmed by a self-consistent numerical calculation.

PACS numbers: 74.78.Bz, 74.78.Fk, 74.45.+c

I. INTRODUCTION

Among many possible types of unconventional superconductors,¹ the materials with the d -wave symmetry of the pair potential are most widely discussed. The d -wave symmetry is established in the quasi-two-dimensional high-temperature cuprate superconductors.^{2,3} A characteristic property of the d -wave superconductivity is the gapless spectrum of quasiparticles. The pair potential is anisotropic, and the gap vanishes along the nodal directions. Another source of low-energy quasiparticles is the surface, which leads to forming the midgap states (MGS);⁴ this phenomenon is due to the change of the sign of the pair potential along a trajectory upon reflection. Thus a d -wave superconductor is a gapless superconductor with two types of low-energy quasiparticles.

The d -wave superconductors can be employed in novel types of logic elements, qubits;^{5,6} there is experimental progress in this direction.^{7,8} However, the low-energy quasiparticles introduce decoherence in d -wave qubits.^{9,10} At the same time, the authors of Ref. 5 mention a possibility to suppress the low-energy quasiparticles due to the finite size of the d -wave banks.

In this paper, we study the influence of the finite size of a d -wave superconductor on the low-energy density of states (DoS) at the surface. There is only a limited number of results related to this issue. The angle-averaged surface DoS was numerically studied by Nagato and Nagai for 45° -oriented superconductors.¹¹ There is also a number of numerical results on the DoS in clean SN systems (where S is a conventional s -wave superconductor and N is a normal metal), which can be relevant to the nodal directions of finite-size d -wave superconductors due to similarity of the pair potential profile along quasiparticle trajectories in the two systems (see below

for details). The works by van Gelder¹² and Gallagher¹³ are the most relevant in this respect. In Ref. 14, Shelankov and Ozana suggested a method to treat multiple-interface superconducting systems and, as an application, numerically considered the DoS in a finite-size bilayer. Their results are relevant for the 45° trajectory in the d -wave system. Finally, we mention an analytical result of Ref. 15, where Fauchère *et al.* considered an SN system with repulsive interaction between the electrons in the N layer. In our language, their result refers to the splitting of the MGS.

We demonstrate that the continuous normal-metallic spectrum along the nodal directions transforms to a set of energy bands; the lowest band is separated from zero by a gap. The midgap states (existing in the finite intervals of the trajectory angles $45^\circ - \alpha < |\theta| < 45^\circ + \alpha$ — see Fig. 1 for notations) transform to two energy bands, situated symmetrically around zero, thus a gap appears. This gap depends on the direction of the quasiparticle trajectory, and vanishes for exactly $\theta = 45^\circ$ direction (at any crystalline orientation α). After averaging over the directions, the DoS is zero at zero energy, and behaves linearly at small energies. Thus the averaged surface DoS remains gapless but is strongly suppressed compared to that in the bulk d -wave superconductor (i.e., at $L \rightarrow \infty$).

In Sec. II, we present analytical results for the DoS. In Sec. III, we confirm and illustrate these results by self-consistent numerical calculations. Finally, we present our conclusions in Sec. IV.

II. ANALYTICAL RESULTS

We consider a quasi-two-dimensional $d_{x^2-y^2}$ -wave superconductor of finite width, i.e., a strip in the ab -plane — see Fig. 1. A quasiparticle trajectory is sequentially

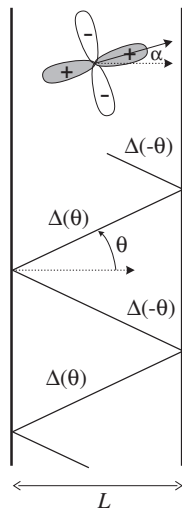


FIG. 1: $d_{x^2-y^2}$ -wave superconductor of finite width L in the ab -plane (quasi-two-dimensional strip). The orientation of the crystalline a -axis with respect to the surface normal is denoted by α , then the angular dependence of the pair potential is $\Delta(\theta) = \Delta_0 \cos(2\theta - 2\alpha)$. The pair potential along the trajectory described by the angle θ changes periodically. We assume $0^\circ \leq \alpha \leq 45^\circ$ — this interval covers all physically different situations.

reflected from one or the other surface of the strip, and the pair potential felt by the quasiparticle changes periodically. The profile of the pair potential along the trajectory is schematically depicted in Fig. 2. This profile is not self-consistent, while the self-consistent pair potential is suppressed near the surfaces (see Sec. III below). However, the width of the regions where this happens has the characteristic scale of the coherence length $\xi = v_F/2\pi T_c$ (v_F is the Fermi velocity, T_c is the superconducting critical temperature¹⁶). We assume $L \gg \xi$, then the regions where Δ is suppressed are relatively narrow, hence the piecewise constant Δ , depicted in Fig. 2, is a good approximation. The results of self-consistent numerical calculations will be discussed below in Sec. III; they agree with the analytical results of the present section.

The real-energy Eilenberger equations along the trajectory have the form (we choose Δ to be real)¹⁷

$$\begin{aligned} \left(-2iE + v_F \frac{\partial}{\partial x}\right) f - 2\Delta g &= 0, \\ \left(-2iE - v_F \frac{\partial}{\partial x}\right) \bar{f} - 2\Delta g &= 0, \\ v_F \frac{\partial}{\partial x} g + \Delta(\bar{f} - f) &= 0, \end{aligned} \quad (1)$$

with the normalization condition

$$g^2 + f\bar{f} = 1. \quad (2)$$

Here g is the normal Green function, while f and \bar{f} are the anomalous Green functions that describe the superconductivity.

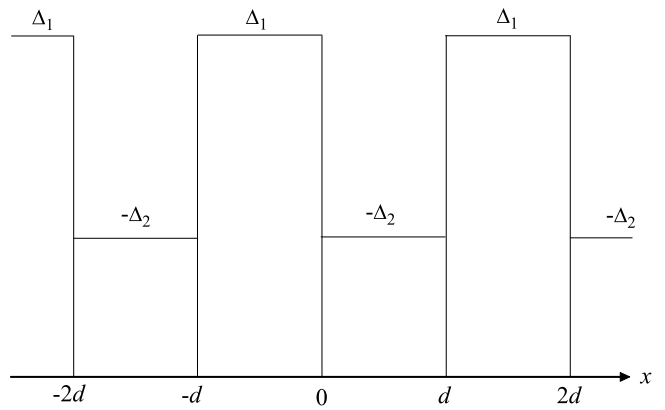


FIG. 2: The pair potential profile along a trajectory in the d -wave superconductor of finite width. The signs are chosen in such a way that the midgap states exist at $\Delta_1, \Delta_2 > 0$. For definiteness, we choose $\Delta_1 \geq \Delta_2$; this does not impose any restrictions on the results. The pair potential changes on the surfaces of the superconductor. With respect to Fig. 1, the introduced notations are defined as $\Delta_1 = \Delta(\theta)$, $\Delta_2 = -\Delta(-\theta)$, and $d = L/\cos\theta$.

Since the Green functions along the trajectory are continuous upon specular reflection at the surfaces of the d -wave superconductor, they obey the same condition in the effective one-dimensional problem described by Fig. 2: g , f , and \bar{f} must be continuous at the edges of the intervals of constant Δ .

The DoS (normalized by its normal-metal value) is determined by the real part of the normal Green function:

$$\nu = \text{Re } g. \quad (3)$$

The DoS is symmetric, $\nu(E) = \nu(-E)$.

In the bulk, the Green functions are

$$g = \frac{-iE}{\sqrt{\Delta^2 - E^2}}, \quad f = \bar{f} = \frac{\Delta}{\sqrt{\Delta^2 - E^2}}, \quad (4)$$

which yields the standard DoS

$$\nu = \text{Re} \frac{|E|}{\sqrt{E^2 - \Delta^2}}. \quad (5)$$

The general solution of the Eilenberger equations (1) is

$$\begin{aligned} \begin{pmatrix} g \\ f \\ \bar{f} \end{pmatrix} &= A \begin{pmatrix} -iE \\ \Delta \\ \Delta \end{pmatrix} + \frac{B}{2} \begin{pmatrix} iE + \sqrt{\Delta^2 - E^2} \\ iE - \sqrt{\Delta^2 - E^2} \end{pmatrix} e^{kx} \\ &+ \frac{C}{2} \begin{pmatrix} \Delta \\ iE - \sqrt{\Delta^2 - E^2} \\ iE + \sqrt{\Delta^2 - E^2} \end{pmatrix} e^{-kx}, \end{aligned} \quad (6)$$

with

$$k = \frac{2\sqrt{\Delta^2 - E^2}}{v_F}. \quad (7)$$

The normalization condition (2) yields:

$$A^2 + BC = \frac{1}{\Delta^2 - E^2}. \quad (8)$$

When the pair potential is spatially symmetric, $\Delta(x) =$

$\Delta(-x)$, the Green functions obey the relations $g(x) = g(-x)$, $f(x) = \bar{f}(-x)$, hence $B = C$. In our case, the pair potential is symmetric with respect to the center of each interval, thus we can write

$$\begin{pmatrix} g \\ f \end{pmatrix} = A_1 \begin{pmatrix} -iE \\ \Delta_1 \end{pmatrix} + B_1 \begin{pmatrix} \Delta_1 \cosh(k_1(x + d/2)) \\ iE \cosh(k_1(x + d/2)) + \sqrt{\Delta_1^2 - E^2} \sinh(k_1(x + d/2)) \end{pmatrix} \quad (9)$$

at $-d < x < 0$, and

$$\begin{pmatrix} g \\ f \end{pmatrix} = A_2 \begin{pmatrix} -iE \\ -\Delta_2 \end{pmatrix} + B_2 \begin{pmatrix} -\Delta_2 \cosh(k_2(x - d/2)) \\ iE \cosh(k_2(x - d/2)) + \sqrt{\Delta_2^2 - E^2} \sinh(k_2(x - d/2)) \end{pmatrix} \quad (10)$$

at $0 < x < d$, while the solution on all the other intervals is obtained due to $2d$ -periodicity of the Green functions.

The boundary conditions (continuity of the Green functions) at $x = 0$ and $x = d$ yield four equations, only three of which are independent. Solving this system of equations and using the normalization condition (8), we determine all the four coefficients A_1 , A_2 , B_1 , and B_2 . Then we find the Green functions and the DoS at the interface between the two intervals (this corresponds to the surface DoS in the d -wave superconductor):

$$\nu(x=0) = \text{Re} \frac{E \left[\sqrt{\Delta_1^2 - E^2} \tanh\left(\frac{k_2 d}{2}\right) + \sqrt{\Delta_2^2 - E^2} \tanh\left(\frac{k_1 d}{2}\right) \right]}{\sqrt{\left(\frac{\sqrt{\Delta_1^2 - E^2} \sqrt{\Delta_2^2 - E^2}}{\cosh(k_1 d/2) \cosh(k_2 d/2)} \right)^2 - \left[(E^2 + \Delta_1 \Delta_2) \tanh\left(\frac{k_1 d}{2}\right) \tanh\left(\frac{k_2 d}{2}\right) - \sqrt{\Delta_1^2 - E^2} \sqrt{\Delta_2^2 - E^2} \right]^2}}. \quad (11)$$

A similar formula was obtained by Gallagher;^{13,18} at the same time, our results are different since his formula refers to the center of the strip in the d -wave problem, while we study the surface DoS.

The zero-energy DoS can be found immediately. If $\Delta_1 \neq \Delta_2$, then Eq. (11) yields $\nu(E=0) = 0$. If $\Delta_1 = \Delta_2$ ($\equiv \Delta$), then we obtain

$$\nu(E=0) = \cosh\left(\frac{\Delta d}{v_F}\right). \quad (12)$$

In the above calculations, we did not assume $\Delta d/v_F \gg 1$, however it is necessary to assume this in order to make the results physically sound, because in a d -wave superconductor, the piecewise constant pair potential (see Fig. 2) is a good approximation only under this condition.

Below we analyze Eq. (11) at low energies, $E \ll \Delta$, in the following relevant cases: a) $\Delta_2 = 0$ (nodal directions), b) $\Delta_1 \neq \Delta_2$, and c) $\Delta_1 = \Delta_2$ (the latter two cases correspond to the presence of the MGS in the infinite system).

A. Effect of the finite size on the nodal quasiparticles

Let us consider a nodal direction, which corresponds to $\Delta_2 = 0$. For brevity, we shall denote Δ_1 by Δ .

In the bulk, the DoS along a nodal direction is normal-metallic,

$$\nu_{d \rightarrow \infty} = 1. \quad (13)$$

The finite-size problem was considered previously (although in a different context) by van Gelder¹² and Gallagher.¹³ While van Gelder considered an academic one-dimensional model with periodic step function $\Delta(x)$, in the work by Gallagher this situation emerged along a quasiparticle trajectory in a superconductor-normal-metal sandwich (with conventional s -wave superconductor). They numerically demonstrated that in this superconducting version of the Kronig-Penney model,¹⁹ the quasiparticle spectrum consists of energy bands with square-root singularities at the band edges. Below we present analytical results for this problem.

Taking into account that

$$\frac{\Delta d}{v_F} \gg 1, \quad (14)$$

$$E \ll \Delta, \quad (15)$$

we obtain from Eq. (11):

$$\nu = \text{Re} \frac{\Delta \sin\left(\frac{Ed}{v_F}\right) + E \cos\left(\frac{Ed}{v_F}\right)}{\sqrt{-\left[E \sin\left(\frac{Ed}{v_F}\right) - \Delta \cos\left(\frac{Ed}{v_F}\right) + 2\Delta \exp\left(-\frac{\Delta d}{v_F}\right)\right] \left[E \sin\left(\frac{Ed}{v_F}\right) - \Delta \cos\left(\frac{Ed}{v_F}\right) - 2\Delta \exp\left(-\frac{\Delta d}{v_F}\right)\right]}}. \quad (16)$$

The bands are situated around the energies at which $E \sin(Ed/v_F) - \Delta \cos(Ed/v_F) = 0$. Since we consider $E \ll \Delta$, then $\cos(Ed/v_F)$ must be very small to fulfill this equation, hence its argument is very close to $\pi/2$ (for the lowest band). Thus the center of the lowest band is

$$E_0 = \frac{\pi v_F}{2 d} \left(1 - \frac{v_F}{\Delta d}\right) \approx \frac{\pi v_F}{2 d}. \quad (17)$$

In the vicinity of E_0 , the DoS can be written as

$$\nu = \text{Re} \frac{v_F/d}{\sqrt{-\left[E - E_0 + 2\frac{v_F}{d} \exp\left(-\frac{\Delta d}{v_F}\right)\right] \left[E - E_0 - 2\frac{v_F}{d} \exp\left(-\frac{\Delta d}{v_F}\right)\right]}}}, \quad (18)$$

hence the width of the band is

$$\delta E = 4 \frac{v_F}{d} \exp\left(-\frac{\Delta d}{v_F}\right), \quad (19)$$

and the DoS has integrable square-root singularities at the edges of the band.

The minimal value of the DoS in the band is achieved at $E = E_0$, and equals

$$\nu_{\min} = \frac{1}{2} \exp\left(\frac{\Delta d}{v_F}\right). \quad (20)$$

The physical mechanisms behind the above results are quite transparent. Instead of the normal-metallic situation that takes place for the nodal directions in the bulk, in the finite system we obtain the profile of the pair potential corresponding to the SN superlattice (Fig. 2 with $\Delta_2 = 0$). Then the energy spectrum in each normal layer consists of the Andreev levels²⁰ which are smeared into the bands due to periodicity of the system. The energy of the lowest Andreev level corresponds to the center of the band, see Eq. (17), while smearing is due to tunneling across the barrier of height Δ and width d , and thus contains the tunneling exponential, see Eq. (19).

B. Effect of the finite size on the midgap states

In the infinite system ($L, d \rightarrow \infty$), the midgap states arise if the pair potential changes its sign upon reflection

from the surface.⁴ According to our definitions (Figs. 1 and 2), this happens at $\Delta_1, \Delta_2 > 0$. The MGS are localized near the surfaces and have exactly zero energy; the corresponding DoS is

$$\nu_{d \rightarrow \infty} = 2\pi \frac{\Delta_1 \Delta_2}{\Delta_1 + \Delta_2} \delta(E). \quad (21)$$

Below we consider the effect of finite d on this result; the results for the cases of differing and coinciding Δ_1 and Δ_2 will be qualitatively different.

1. The case $\Delta_1 > \Delta_2$

Let us consider the general case, when Δ_1 and Δ_2 are nonzero and can be different (still, the signs are such that the MGS exist in the infinite system). Employing

$$\frac{\Delta_1 d}{v_F}, \frac{\Delta_2 d}{v_F} \gg 1, \quad (22)$$

$$E \ll \Delta_1, \Delta_2, \quad (23)$$

and expanding Eq. (11), we obtain:

$$\nu = \frac{2\Delta_1\Delta_2}{\Delta_1 + \Delta_2} \operatorname{Re} \frac{E}{\sqrt{-\left[E^2 - \left(\frac{2\Delta_1\Delta_2}{\Delta_1 + \Delta_2}\right)^2 (e_2 - e_1)^2\right] \left[E^2 - \left(\frac{2\Delta_1\Delta_2}{\Delta_1 + \Delta_2}\right)^2 (e_2 + e_1)^2\right]}}, \quad (24)$$

$$e_1 = \exp\left(-\frac{\Delta_1 d}{v_F}\right), \quad e_2 = \exp\left(-\frac{\Delta_2 d}{v_F}\right).$$

This yields two bands, situated symmetrically around zero energy. The edges of the positive-energy band are

$$E_{b,\min} = \frac{2\Delta_1\Delta_2}{\Delta_1 + \Delta_2} \left[\exp\left(-\frac{\Delta_2 d}{v_F}\right) - \exp\left(-\frac{\Delta_1 d}{v_F}\right) \right], \quad (25)$$

$$E_{b,\max} = \frac{2\Delta_1\Delta_2}{\Delta_1 + \Delta_2} \left[\exp\left(-\frac{\Delta_2 d}{v_F}\right) + \exp\left(-\frac{\Delta_1 d}{v_F}\right) \right]. \quad (26)$$

The minimal value of the DoS in the band is achieved at $E = \frac{2\Delta_1\Delta_2}{\Delta_1 + \Delta_2} \sqrt{e_2^2 + e_1^2}$, and equals

$$\nu_{\min} = \frac{1}{2} \sqrt{\frac{1}{e_1^2} + \frac{1}{e_2^2}} \sim \frac{1}{2} \exp\left(\frac{\Delta_1 d}{v_F}\right). \quad (27)$$

At the edges of the bands, the DoS has integrable square-root singularities.

The position of the center of the band in the limit $\Delta_1 \gg \Delta_2$ was calculated in Ref. 15 (although in a different context), while only discrete energy levels were discussed and the width of the band was not studied.

Physically, the obtained results can be explained as follows. In the infinite system, $d \rightarrow \infty$, we have the zero-energy levels localized near the interfaces between Δ_1 and $-\Delta_2$. The first effect of the finite d is to split the levels at the two neighboring interfaces due to tunneling across the Δ_2 barrier (the lowest barrier). This splitting is symmetric with respect to zero energy. Physically, it is similar to the standard quantum-mechanical problem of the level splitting in the double-well potential.²¹ The second effect of the finite d is to smear each of the split levels due to periodicity of the system; the smearing is due to tunneling across the Δ_1 barriers. This is similar to the standard Kronig–Penney model.¹⁹ As a result, the center of the band (25)–(26) is determined by the tunneling exponential containing Δ_2 , while the width of the band is determined by the tunneling exponential containing Δ_1 . Since $\Delta_2 < \Delta_1$, the splitting of the zero-energy level is larger than its smearing, hence a gap in the spectrum arises.

2. The case $\Delta_1 = \Delta_2$

At $\Delta_1 = \Delta_2$ ($\equiv \Delta$), the DoS (24) reduces to

$$\nu = \frac{\Delta}{\sqrt{E_b^2 - E^2}}, \quad E_b = 2\Delta \exp\left(-\frac{\Delta d}{v_F}\right). \quad (28)$$

Thus the MGS is smeared into the band of width $2E_b$ around zero. The minimal value of the DoS is achieved at $E = 0$, and equals

$$\nu_{\min} = \frac{1}{2} \exp\left(\frac{\Delta d}{v_F}\right), \quad (29)$$

while at the edges of the band (at $E = \pm E_b$), the DoS has integrable square-root singularities.

This result means that the two bands (positive and negative) that existed at $\Delta_1 > \Delta_2$, touch each other at $E = 0$ and merge into a single band, while the singularities at $E = 0$ transform into the minimum (29). The equivalent result about the band centered at $E = 0$ was numerically obtained in Ref. 14 (although in a different context).

The physical explanation of these results is the same as in the previous case, $\Delta_1 > \Delta_2$. The only difference is that in the case of equal barriers, $\Delta_1 = \Delta_2$, the splitting of the zero-energy level is exactly the same as its smearing, hence no gap in the spectrum appears.

C. Angle-averaged DoS

Let us consider the behavior of the angle-averaged surface DoS at $E \rightarrow 0$. The only contribution to the DoS arises from the vicinity of the angles at which $\Delta_1 = \Delta_2$ — these are always the $\theta = \pm 45^\circ$ angles [at any orientation α , since $\Delta(\theta) = \Delta_0 \cos(2\theta - 2\alpha)$].

Introducing ϑ via $\theta = \pi/4 - \vartheta$, we expand the pair potential in the vicinity of $\theta = 45^\circ$:

$$\Delta_1 \approx \Delta + \Delta' \vartheta, \quad \Delta_2 \approx \Delta - \Delta' \vartheta, \quad (30)$$

where

$$\Delta = \Delta_0 \sin 2\alpha, \quad \Delta' = 2\Delta_0 \cos 2\alpha. \quad (31)$$

Then we expand

$$e_2 - e_1 \approx \exp\left(-\frac{\Delta d}{v_F}\right) \frac{2\Delta' \vartheta d}{v_F} \quad (32)$$

— we assume that

$$\frac{\Delta' \vartheta d}{v_F} \ll 1 \quad (33)$$

(since $\Delta' \sim \Delta$, this condition implies that $\vartheta \ll v_F/\Delta d \ll 1$). The angle-resolved DoS (24) then takes the form

$$\nu = \Delta \operatorname{Re} \frac{E}{\sqrt{-\left\{E^2 - \left[\frac{2\Delta\Delta'd}{v_F} \exp\left(-\frac{\Delta d}{v_F}\right)\right]^2\right\} \left\{E^2 - \left[2\Delta \exp\left(-\frac{\Delta d}{v_F}\right)\right]^2\right\}}}. \quad (34)$$

The contribution to the angle-averaged DoS comes from the interval $-\vartheta_b < \vartheta < \vartheta_b$, where

$$\vartheta_b = \frac{E}{\frac{2\Delta\Delta'd}{v_F} \exp\left(-\frac{\Delta d}{v_F}\right)}. \quad (35)$$

Condition (33) for all ϑ up to ϑ_b is equivalent to

$$E \ll E_b, \quad (36)$$

where $E_b = 2\Delta \exp(-\Delta d/v_F)$ is the upper edge of the band.

The angle-resolved DoS (34) can be written as

$$\nu = \frac{1}{\frac{4\Delta\Delta'd}{v_F} \exp\left(-\frac{2\Delta d}{v_F}\right)} \operatorname{Re} \frac{E}{\sqrt{\vartheta_b^2(E) - \vartheta^2}}. \quad (37)$$

The angle-averaged DoS is

$$\nu_{\text{av}} = \frac{2}{\pi} \int_{-\vartheta_b}^{\vartheta_b} \nu(\vartheta) d\vartheta = \frac{E}{\frac{2\Delta\Delta'd}{v_F} \exp\left(-\frac{2\Delta d}{v_F}\right)}. \quad (38)$$

The DoS is zero at zero energy, and behaves linearly at small E . Thus the averaged surface DoS remains gapless but is strongly suppressed compared to that in the bulk d -wave superconductor (i.e., at $L \rightarrow \infty$).

The gapless structure of the angle-averaged DoS (38) is due to integrating in the vicinity of $\theta = \pm 45^\circ$, where the gap in the angle-resolved DoS vanishes. At the same time, the DoS probed by transport methods²² is given by

$$\nu_{\text{tr}} \sim \int \nu(\theta) D(\theta) d\theta, \quad (39)$$

and differs from Eq. (38) by the weighting factor $D(\theta)$, the angle-dependent transparency of the tunneling interface. When the tunneling interface has finite thickness, the function $D(\theta)$ is exponentially suppressed at not too small θ , then the contribution of the $\theta = \pm 45^\circ$ trajectories can be significantly suppressed [since $\nu_{\text{tr}} \sim D(45^\circ)\nu_{\text{av}}$ at low energies]. In this case, we can expect that the transport DoS ν_{tr} will be gapped despite the angular averaging. The directional selectivity of tunneling is most pronounced in the scanning tunneling spectroscopy experiments, where the effective tunneling cone around the surface normal can be as narrow as $\delta\theta \sim 20^\circ$.²³

The result (38) for the angle-averaged DoS does not refer to the cases $\alpha = 0^\circ$ and $\alpha = 45^\circ$ (and close orientations); these cases are special.

At $\alpha = 0^\circ$, the MGS do not appear, and the low-energy DoS is entirely due to the nodal directions. Then according to Sec. II A, the spectrum along a nodal direction acquires a gap due to the finite size. In this situation, the angular averaging preserves the gap in the spectrum, approximately given by Eq. (17).

At $\alpha = 45^\circ$, the condition $\Delta_1 = \Delta_2$ (which implies the gapless spectrum) is satisfied not only at $\theta = \pm 45^\circ$ but at any θ (all trajectories). Then angular averaging does not introduce new qualitative features (compared to the angle-resolved result), and the DoS at small energies is large according to the results of Sec. II B 2. Comparing with the bulk case, we can say that due to the finite size, the zero-energy peak in the DoS is smeared but not split. This statement agrees with the results of Nagato and Nagai¹¹ who studied this case by a self-consistent numerical method.

The above results refer to the surface DoS. However, the averaged DoS is linear at low energies also inside the strip, although the slope is different from Eq. (38), because the MGS contributing to this result decay into the bulk of the sample. For example, in the middle of the strip the angle-averaged DoS differs from Eq. (38) by an additional factor $2 \exp(-\Delta d/v_F)$. This result is again valid at $E \ll E_b$; this interval shrinks in the limit of large d , where the DoS is mainly determined by the standard nodal contribution at larger E .

III. SELF-CONSISTENT NUMERICAL RESULTS

In order to take into account the spatial inhomogeneity of the pair potential, we solve the problem numerically by a self-consistent numerical method similar to the one used in Ref. 24. We rewrite the Eilenberger equations employing the Riccati parametrization,²⁵ which is well suited for numerical integration. Starting from the spatially homogeneous pair potential, we calculate the Green functions over the whole sample, and then use the self-consistency equation to refine the initial approximation for the pair potential. The procedure is repeated iteratively until the necessary accuracy is reached.

An example of the pair potential along a trajectory, calculated self-consistently, is shown in Fig. 3. In anisotropic superconductors, surfaces lead to pair breaking and suppression of the pair potential. The region where the suppression takes place, has the characteristic scale of ξ , hence at $L \gg \xi$ the piecewise constant Δ (see Fig. 2) is a good approximation.

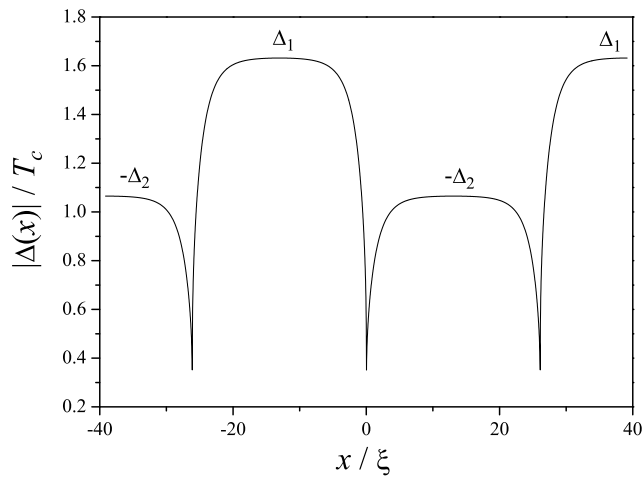


FIG. 3: Self-consistent profile of the pair potential along the $\theta = 40^\circ$ trajectory at the crystalline orientation $\alpha = 20^\circ$. The width of the d -wave strip is $L = 20\xi$, the length of the trajectory between the successive reflections from the surfaces is $d = L/\cos 40^\circ$.

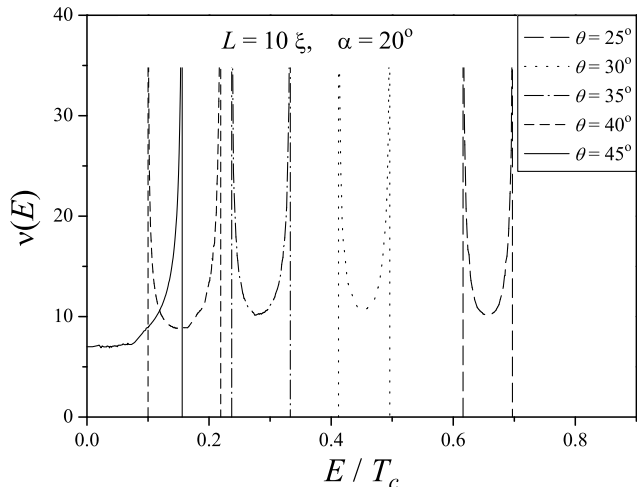


FIG. 4: The low-energy angle-resolved DoS for several trajectories θ at the width of the strip $L = 10\xi$ and the crystalline orientation $\alpha = 20^\circ$.

Figures 4 and 5 demonstrate the angle-resolved DoS for two values of the strip width: $L = 10\xi$ and $L = 20\xi$. These numerical results agree with the analytical theory developed in Sec. II. Indeed, we observe that the spectrum consists of the energy bands, both along the nodal direction ($\theta = 25^\circ$)²⁶ and the directions for which the MGS exist in the limit $L \rightarrow \infty$ ($\theta = 30^\circ, 35^\circ, 40^\circ$, and 45°). The DoS is minimal in the centers of the bands and demonstrates the square-root singularities on their edges.

The energy gap for the lowest band along the nodal direction ($\theta = 25^\circ$) is larger than for the MGS directions; this agrees with our analytical results according to which the gap for the nodal direction does not contain an exponentially small factor [see Eq. (17) and note that

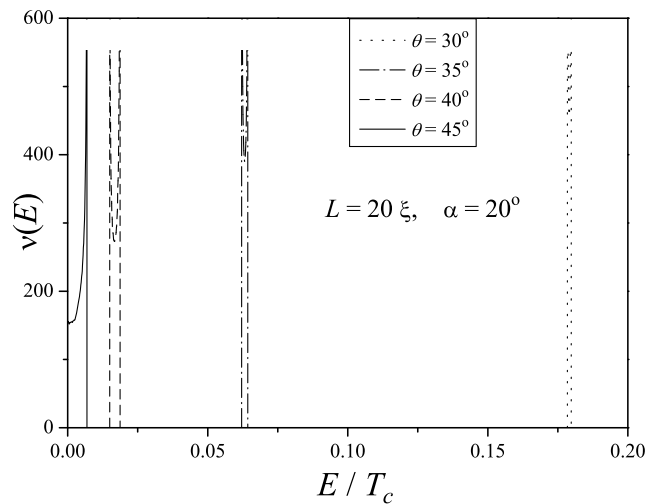


FIG. 5: The same as in Fig. 4 but for $L = 20\xi$.

the energy gap is of the same order as the center of the band since the width of the band is much smaller]. The lowest energy band for the nodal direction can be seen in Fig. 4, while in Fig. 5 it is beyond the demonstrated energy range.

The energy bands for the MGS directions are gapped if $\theta \neq 45^\circ$, which corresponds to the case $\Delta_1 \neq \Delta_2$ studied in Sec. II B 1. The $\theta = 45^\circ$ direction corresponds to the case $\Delta_1 = \Delta_2$ studied in Sec. II B 2; the energy band is gapless in this case, its center is $E = 0$ where the DoS reaches a minimum.

As L increases, the energy gaps become smaller and the bands become narrower.

The numerical results allow us to directly check the accuracy of our analytical estimates. For example, we consider the $\theta = 40^\circ$ direction at $L = 20\xi$. Then the edges of the energy band are given by Eqs. (25) and (26) which yield the center of the band $E_0/T_c = 0.015$ and the width of the band $\delta E/T_c = 0.0029$, while the numerical results are $E_0/T_c = 0.017$ and $\delta E/T_c = 0.0037$ (see Fig. 5). Thus we conclude that our analytical results provide reasonable quantitative accuracy while capturing all qualitative features of the DoS.

IV. CONCLUSIONS

We have considered the effect of the finite size in the ab -plane on the density of states (DoS) in d -wave superconductors. We assumed finiteness in one direction, thus we deal with quasi-two-dimensional strip instead of quasi-two-dimensional plane. We assumed arbitrary crystalline orientation, described by the angle α between the a -axis and the normal to the surfaces.

The problem is solved analytically neglecting the suppression of the pair potential near the surfaces; the results are confirmed by a self-consistent numerical calculation.

In the relevant limits, our results agree with previous studies.

In the bulk, the DoS is gapless along the nodal directions, while the presence of a surface leads to formation of another type of the low-energy states, the midgap states with zero energy. Due to the finite size of the superconductor, the spectrum of nodal quasiparticles acquires an energy gap. The midgap states acquire the angle-dependent gap that vanishes at $\theta = 45^\circ$ (θ is the angle between the trajectory and the normal to the surface); this result is valid unless the crystal is 0° - or 45° -oriented ($\alpha \neq 0^\circ$ or 45°). In the special case of $\alpha = 0^\circ$, the midgap states are absent, and the spectrum is gapped for all trajectories (including the nodal directions). On the opposite, in the case of $\alpha = 45^\circ$, the spectrum is gapless for all trajectories θ . In all the cases, the angle-resolved DoS consists of energy bands that are formed similarly to the Kronig–Penney model.

In the special case of $\alpha = 0^\circ$, the angle-averaged DoS has a gap. In the special case of $\alpha = 45^\circ$, the angle-averaged DoS is finite at low energies.

At $\alpha \neq 0^\circ$ or 45° , the angle-averaged surface DoS is strongly suppressed due to finite size, while remains gapless and behaves linearly at small energies. The low-energy contribution comes from the trajectories with $\theta \approx 45^\circ$, hence we can expect that the energy gap survives upon angular averaging if one measures the *transport* DoS in the case when the 45° -angle contribution is suppressed by the transparency of the tunneling barrier.

In our model, we did not take into account such imperfections in the system as bulk impurities^{27,28,29,30,31} and interface roughness.^{32,33,34} We expect them to smear the features discussed in the present paper. In particular, the energy bands (in the angle-resolved DoS) sepa-

rated from zero by gaps, exist only when imperfections are weak, otherwise the bands are smeared and finite DoS appears at zero energy. A rough estimate demonstrates that smearing of the bands due to the bulk impurities exceeds the width of the bands if the electronic mean free path l is smaller than the width of the strip L . However, the effects discussed above can survive in the case of rare impurities, when $l \gg L$ and long intervals along the strip (between two neighboring impurities) can be considered clean.

Our model is not material-specific and can be in principle applied to any d -wave superconductor. However, the only class of materials where the d -wave symmetry is established at present, is the high- T_c oxides, where the coherence length ξ is very small. Then the finite-size effects discussed above become pronounced at quite small size L .

Acknowledgments

We are grateful to M. H. S. Amin, Yu. S. Barash, A. M. Bobkov, I. V. Bobkova, M. V. Feigel'man, M. Yu. Kupriyanov, G. Leibovitch, and A. M. Zagoskin for helpful discussions. The research was supported by the D-Wave Systems Inc. and the ESF PiShift program. Ya.V.F. was also supported by the RFBR grants Nos. 03-02-16677 and 04-02-16348, the Russian Science Support Foundation, the Russian Ministry of Industry, Science and Technology, the program “Quantum Macrophysics” of the Russian Academy of Sciences, CRDF, and the Russian Ministry of Education.

* Electronic address: fominov@landau.ac.ru

† Electronic address: a.golubov@tnw.utwente.nl

¹ V. P. Mineev and K. V. Samokhin, *Introduction to Unconventional Superconductivity* (Gordon & Breach, Amsterdam, 1999).

² D. J. Van Harlingen, *Rev. Mod. Phys.* **67**, 515 (1995).

³ C. C. Tsuei and J. R. Kirtley, *Rev. Mod. Phys.* **72**, 969 (2000).

⁴ C.-R. Hu, *Phys. Rev. Lett.* **72**, 1526 (1994).

⁵ L. B. Ioffe, V. B. Geshkenbein, M. V. Feigel'man, A. L. Fauchère, and G. Blatter, *Nature (London)* **398**, 679 (1999).

⁶ A. M. Zagoskin, cond-mat/9903170 (1999); A. Blais and A. M. Zagoskin, *Phys. Rev. A* **61**, 042308 (2000).

⁷ E. Il'ichev, M. Grajcar, R. Hlubina, R. P. J. IJsselsteijn, H. E. Hoening, H.-G. Meyer, A. Golubov, M. H. S. Amin, A. M. Zagoskin, A. N. Omelyanchouk, and M. Yu. Kupriyanov, *Phys. Rev. Lett.* **86**, 5369 (2001).

⁸ A. Ya. Tzalenchuk, T. Lindström, S. A. Charlebois, E. A. Stepantsov, Z. Ivanov, A. M. Zagoskin, *Phys. Rev. B* **68**, 100501(R) (2003).

⁹ Ya. V. Fominov, A. A. Golubov, and M. Yu. Kupriyanov,

Pis'ma Zh. Éksp. Teor. Fiz. **77**, 691 (2003) [*JETP Lett.* **77**, 587 (2003)].

¹⁰ M. H. S. Amin and A. Yu. Smirnov, *Phys. Rev. Lett.* **92**, 017001 (2004).

¹¹ Y. Nagato and K. Nagai, *Phys. Rev. B* **51**, 16254 (1995).

¹² A. P. van Gelder, *Phys. Rev.* **181**, 787 (1969).

¹³ W. J. Gallagher, *Phys. Rev. B* **22**, 1233 (1980).

¹⁴ A. Shelankov and M. Ozana, *Phys. Rev. B* **61**, 7077 (2000).

¹⁵ A. L. Fauchère, W. Belzig, and G. Blatter, *Phys. Rev. Lett.* **82**, 3336 (1999).

¹⁶ The zero-temperature amplitude of the pair potential in the bulk is related to the critical temperature as $\Delta_0 = 2.14T_c$, where the amplitude Δ_0 is defined so that $\Delta(\theta) = \Delta_0 \cos(2\theta - 2\alpha)$.

¹⁷ G. Eilenberger, *Z. Phys.* **214**, 195 (1968).

¹⁸ It is interesting to note that Gallagher solved the Gor'kov equations with subsequent averaging over spatial oscillations on the scale of $1/k_F$ (k_F is the Fermi wavevector), while we start from the quasiclassical Eilenberger equations. Thus the correspondence between our results implies that the quasiclassical approximation in the problem is valid provided $k_F L \gg 1$.

- ¹⁹ R. de L. Kronig and W. Penney, Proc. R. Soc. London, Ser. A **130**, 499 (1931). See also S. Flügge, *Practical Quantum Mechanics I* (Springer-Verlag, Berlin, 1971).
- ²⁰ A. F. Andreev, Zh. Éksp. Teor. Fiz. **46**, 1823 (1964); **49**, 655 (1965) [Sov. Phys. JETP **19**, 1228 (1964); **22**, 455 (1966)]; I. O. Kulik, Zh. Éksp. Teor. Fiz. **57**, 1745 (1969) [Sov. Phys. JETP **30**, 944 (1970)].
- ²¹ L. D. Landau and E. M. Lifshitz, *Quantum Mechanics: Non-Relativistic Theory, Volume 3* (Butterworth-Heinemann, Oxford, 1981).
- ²² Y. Tanaka and S. Kashiwaya, Phys. Rev. Lett. **74**, 3451 (1995).
- ²³ A. Sharoni, G. Leibovitch, A. Kohen, R. Beck, G. Deutscher, G. Koren, and O. Millo, Europhys. Lett. **62**, 883 (2003).
- ²⁴ M. H. S. Amin, A. N. Omelyanchouk, S. N. Rashkeev, M. Coury, and A. M. Zagoskin, Physica B **318**, 162 (2002).
- ²⁵ N. Schopohl and K. Maki, Phys. Rev. B **52**, 490 (1995); N. Schopohl, cond-mat/9804064 (1998).
- ²⁶ At $\alpha = 20^\circ$, one of the nodal directions in the bulk is $\theta = -25^\circ$. In the strip geometry, we call the $\theta = 25^\circ$ direction nodal because the corresponding trajectory includes the nodal $\theta = -25^\circ$ segments (see Fig. 1).
- ²⁷ P. J. Hirschfeld, P. Wölfle, and D. Einzel, Phys. Rev. B **37**, 83 (1988).
- ²⁸ Yu. S. Barash, A. A. Svidzinskii, and V. P. Mineev, Pis'ma Zh. Éksp. Teor. Fiz. **65**, 606 (1997) [JETP Lett. **65**, 638 (1997)].
- ²⁹ A. Poenicke, Yu. S. Barash, C. Bruder, and V. Istyukov, Phys. Rev. B **59**, 7102 (1999).
- ³⁰ M. L. Kulić and O. V. Dolgov, Phys. Rev. B **60**, 13062 (1999).
- ³¹ Y. Asano, Y. Tanaka, and S. Kashiwaya, cond-mat/0302287 (2003).
- ³² M. Matsumoto and H. Shiba, J. Phys. Soc. Jpn. **64**, 1703 (1995).
- ³³ Yu. S. Barash, A. A. Svidzinsky, and H. Burkhardt, Phys. Rev. B **55**, 15282 (1997).
- ³⁴ A. A. Golubov and M. Yu. Kupriyanov, Pis'ma Zh. Éksp. Teor. Fiz. **69**, 242 (1999) [JETP Lett. **69**, 262 (1999)].